Int. J. Electrochem. Sci., 8 **(2013)** 903 - 913

International Journal of
ELECTROCHEMICAL
SCIENCE
www.electrochemsci.org

PEG-assisted Solid State Synthesis and Characterization of Carbon-Coated Li_2MnSiO_4 Cathode Materials for Lithium Ion Battery

Zhenbo Peng[1,2], He Miao[1], Hongfeng Yin[1], Cheng Xu[1], Wei Guo Wang[1,]*

[1] Ningbo Institute of Material Technology & Engineering (NIMTE),Chinese Academy of Sciences, Ningbo, 315201, P. R. China
[2] Department of Applied Chemical Engineering, Ningbo Polytechnic College, Ningbo, 315800, P.R. China
[*]E-mail: wgwang@nimte.ac.cn

Received: 8 November 2012 / *Accepted:* 17 December 2012 / *Published:* 1 January 2013

Phase-pure carbon-coated Li_2MnSiO_4 cathode material has been prepared through a PEG-assisted solid state reaction strategy. Transmission electron microscopy further confirmed that the Li_2MnSiO_4 nanocrystals (~50nm) were coated with amorphous carbon layer on their surface. The as-obtained Li_2MnSiO_4 cathode material exhibited the most initial discharge capacity of 204 mAh g^{-1} at the 10 mA g^{-1} current density at room temperature and the highest discharge capacity of 128 mAh g^{-1} at the 200 mA g^{-1} current density. Compared with PEG free Li_2MnSiO_4 cathode material, electrochemical performance of Li_2MnSiO_4 with PEG was greatly improved due to the pure phase, reduction in particle size. Influences of calcination temperature and PEG addition on phase purity, surface morphology as well as electrochemical performance were studied in detail, in which it was found that PEG as a dispersant made the slurry more uniform and stable during ball milling process and favored the phase-pure Li_2MnSiO_4.

Keywords: Lithium-ion battery; Cathode material; Li_2MnSiO_4; Solid state synthesis

1. INTRODUCTION

There has been intensive research on cathode materials for high energy density and high power density applications in lithium ion batteries for the next generation of transportation including hybrid electric vehicles (HEV), plug-in hybrid electric vehicles, and electric vehicles (EV). Lithium orthosilicates, Li_2MSiO_4 (M=Fe, Mn, Co and Ni), have recently attracted attention of researchers due to their appealing properties such as high theoretical capacity (>300 mAh g^{-1}), plausible extraction of more than one Li^+ ion per formula unit and high thermal stability through strong Si–O bonding [1-3].

Among them, Li_2FeSiO_4 and Li_2MnSiO_4 were more attractive since they were cost effective and environmental friendly [4-13]. Li_2MnSiO_4 offers higher cell voltage because of the oxidation of the Mn^{3+}/Mn^{4+} couple rather than Fe^{2+}/Fe^{3+} in Li_2FeSiO_4 [14]. However, preliminary study on Li_2MnSiO_4 by Dominko's group in 2006 indicated a reversible insertion/extraction of less than 0.5 lithium ion per formula unit [8]. The major drawback of the silicate family is their characteristically low electronic conductivity, which was up to 3 orders of magnitude lower than that of $LiFePO_4$ [9]. Carbon coating and particle size reduction were found to be effective ways to enhance the electrochemical activity of this material. Most of the studies reported the usage of either solid state or sol–gel route followed by coating of carbon [2,14-22]. However, the practical capacity was much lower than theoretical capacity, especially at high current density. The capacity fade during cycling was difficult to overcome. 100% phase pure Li_2MnSiO_4 has not been prepared. At least one of impurities such as MnO, Mn_2SiO_4, Li_2SiO_3 was found in the reported Li_2MnSiO_4 [2,14-23]. Aravindan et al. [2] synthesized Li_2MnSiO_4 by an adipic acid assisted sol–gel route, but MnO was unavoidable. De Dompablo et al. [20] succeeded to prepare a Li_2MnSiO_4 material in the absence of MnO under various pressure conditions. Nevertheless, the formation of Mn_2SiO_4 could be inevitable. Devaraju [24] et al. reported pure Li_2MnSiO_4 nanoparticles synthesized via a supercritical solvothermal method, but the small peak around $2\theta=35$ shows small amount of MnO impurity. Therefore, more studies are necessary to obtain phase-pure Li_2MnSiO_4 and improve its electrochemical performance.

In olivine phosphates, particularly, $LiFePO_4$, the conducting problem was circumvented by surface modification especially carbon coating, which dramatically improved the cycle and rate performance of the cell. PEG was employed as carbon source in synthesis of $LiFePO_4$ to improve electronic conductivity [25-27]. In this paper, PEG assisted solid-state method was conducted to synthesis carbon coated Li_2MnSiO_4 Nanoparticles. Phase pure Li_2MnSiO_4 was achieved. PEG addition amount and calcination temperature were optimized, and the role of PEG was discussed.

2. EXPERIMENTAL PART

Analytical grades of $LiOH{\cdot}H_2O$ (SCRC,95%), $Mn(CH_3COO)_2$ (SCRC,99%), and $Si(OC_2H_5)_4$ (SCRC,98%) were used as starting materials to synthesis carbon-coated Li_2MnSiO_4 powder by solid-state reaction method. Ethanol and polyethylene glycol (PEG 10000) were employed as ball milling medium. Stoichiometric amounts of the materials were ball-milled for 6 h in a planetary miller with a rotation speed of 450 rpm to form homogeneous slurry. The slurry was dried in vacuum dryer for at 90ºC for 10h and finely ground to obtain uniform precursor. The precursor was calcined at various temperature conditions from 550ºC to 700ºC with 50ºC interval for 15 h in N_2 atmosphere. Thermal studies were carried out by means of thermogravimetric-differential thermal analysis (TG-DTA) using a thermal analyzer system (Pyris Diamond TG/DTA, Perkin-Elmer, USA). The powder was heated at 5ºC/min in N_2 atmosphere. The crystalline structure of the prepared Li_2MnSiO_4 was studied by X-ray diffractometry (D8 Advance, Bruker AXS, Germany) with Cu-Kα as the radiation source. The surface morphological features of the resulting compounds were observed using a field emission scanning electron microscope (FE-SEM, S-4800, Hitachi, Japan). The high resolution transmission electronic

microscopy (HR-TEM, Tecnai F20, FEI, USA) was utilized to study the carbon coating on the surface of Li_2MnSiO_4. The carbon content of Li_2MnSiO_4 material was determined with an elemental analyzer (2400 Series, Perkin-Elmer II,USA). BET surface area of the material was measured by accelerated surface area and porosimetry System(ASAP 2020M, Micromeritics, USA).

Electrochemical performances were evaluated by CR2032-type coin cells with a battery testing system (Neware BTS-2000). The composite cathode was fabricated from a mixture of active material, Polytetrafluoroethylene (PTFE) and conductive carbon black in a weight ratio of 70:20:10. The mixture was pressed into a film with thickness of 100 μm thickness on a roller. The film was dried at 120ºC for 24 h in a vacuum oven, pressed on a stainless-steel mesh which served as the current collector. The coin cell was made up of a cathode and metallic lithium as anode, which was separated by a porous polypropylene film (Celgard 3401). The 1 mol/L $LiPF_6$ in a mixture of ethylene carbonate (EC)/dimethyl carbonate (DMC) (1:1 v/v) was used as electrolyte. The coin cells were assembled in a glove-box full of argon. The cycling studies were carried out between 1.5 and 4.8V at room temperature with constant current density of 10 mA g^{-1} to 200 mA g^{-1}. Electrochemical impedance spectroscopy of the assembled coin cells was recorded in frequency range of 100mHz to 100KHz with an electrochemical workstation (IM6ex , Zahner, Germany).

3. RESULTS AND DISCUSSION

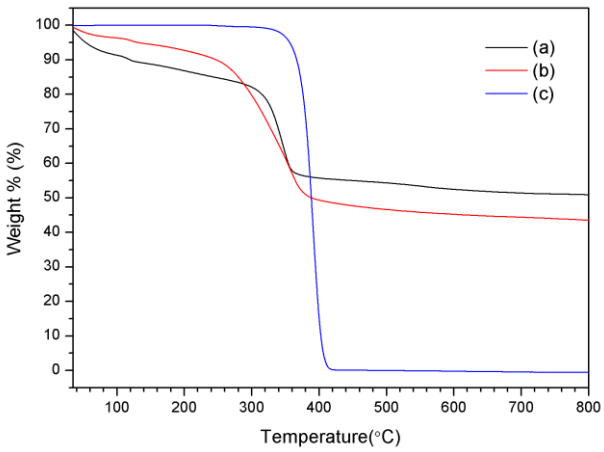

Figure 1. Thermogravimetric (TG) of precursor of Li_2MnSiO_4 in a N_2 atmosphere. (a) precursor of Li_2MnSiO_4 without PEG (b) precursor of Li_2MnSiO_4 with PEG (c) PEG

Thermogravimetric-derivative thermal analysis (TG-DTA) was used to establish the temperature conditions for the synthesis of Li_2MnSiO_4 nanoparticles. Fig. 1 shows the TG curves performed on the precursor of Li_2MnSiO_4. (a) shows the TG curve of precursor of Li_2MnSiO_4 without PEG. (b) shows the TG curve of precursor of Li_2MnSiO_4 with PEG. For the precursor of Li_2MnSiO_4 without PEG, 25% weight loss occurred at 300-360ºC. For the precursor of Li_2MnSiO_4 with PEG, about 40% weight loss occurred at 300-400ºC. As shown in (c), PEG lost almost 100% weight at 380-410ºC. When calcined at 300-380ºC, the source materials decomposed to oxides and formed

amorphous Li_2MnSiO_4 particles. Because decomposition temperature of PEG is higher than that of Li_2MnSiO_4 precursor, the undecomposed PEG is considered to hinder the agglomeration of Li_2MnSiO_4 particles.

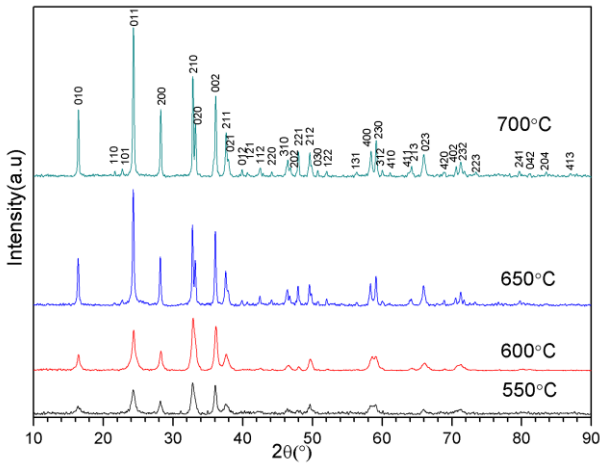

Figure 2. Powder X-ray diffraction patterns of synthesized Li_2MnSiO_4 nanoparticles at various temperatures in N_2 atmosphere.

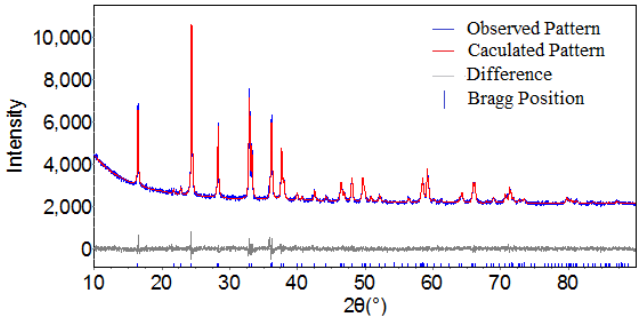

Figure 3. Observed and calculated X-ray diffraction patterns and Bragg positions of Li_2MnSiO_4 prepared at 700ºC

A series of compounds were prepared from 550ºC to 700ºC with the interval of 50ºC in order to optimize the temperature condition for the synthesis of Li_2MnSiO_4 phase. Fig. 2 shows the X-ray diffraction patterns of Li_2MnSiO_4 samples prepared at various temperatures. There are no reflections of the starting materials used for the synthesis. The pattern of sample prepared under 700 ºC shows well defined sharp intense peaks, which are in accordance with the calculated X-ray diagram of Li_2MnSiO_4 proposed by I. Belharouak[9]. The crystalline peaks were indexed according to the orthorhombic structure with P$mn2_1$ group, which is analogous to the Li_3PO_4 pattern[21, 28]. The orthorhombic lattice parameters [a=6.3084Å, b=5.3838 Å, c=4.9690 Å] were refined by Rietveld profile matching and are consistent with values published by others[8,9]. The observed and calculated patterns and the Bragg positions of Li_2MnSiO_4 are shown in Fig.3. Common impurity phase noticed by other researchers

[2,14-23] such as MnO, Li_2SiO_3 and Mn_2SiO_4 were all avoided in our work. The phase pure Li_2MnSiO_4 was firstly prepared by PEG assisted solid-state reaction method. As for the samples prepared at 550ºC, 600ºC and 650ºC, the peaks from XRD patterns are not well-defined, indicating incomplete formation of Li_2MnSiO_4 crystal.

Morphological features of the Li_2MnSiO_4 calcined at different temperatures for 15h are shown in Fig.4. The particles of samples prepared at 550ºC and 600ºC are uniform with the grain size of 30~50 nm. Li_2MnSiO_4 materials prepared at 650ºC and 700ºC exhibit highly aggregated lump like particulate with a wide size range from 20 nm to 200 nm. Calcination temperature greatly influenced the crystallization and the grain size of Li_2MnSiO_4, which are correlated with electronic conductivity [4,14]. Optimization of the temperature was performed based on battery performance of the material. All cells were tested in the voltage range of 1.5-4.8V under a current density of 30mA g^{-1}. The cell performance of the Li_2MnSiO_4 cathode materials prepared under different temperatures was presented in Fig.5. Li_2MnSiO_4 prepared at 550ºC exhibited the initial discharge capacity of 182mAh g^{-1}, but only 33% (60 mAh g^{-1}) retained at the end of 20th cycle due to incomplete phase formation. Li_2MnSiO_4 prepared at 700ºC exhibited the lowest initial discharge capacity of 68 mAh g^{-1} because of severe particles aggregation. Li_2MnSiO_4 prepared at 600ºC delivers the discharge capacity of 180mAh g^{-1} at the second circle, and 59% (103mAh g^{-1}) retained at the end of 20th cycle. From the optimization, 600ºC was found to be the best temperature to accomplish high performance Li_2MnSiO_4.

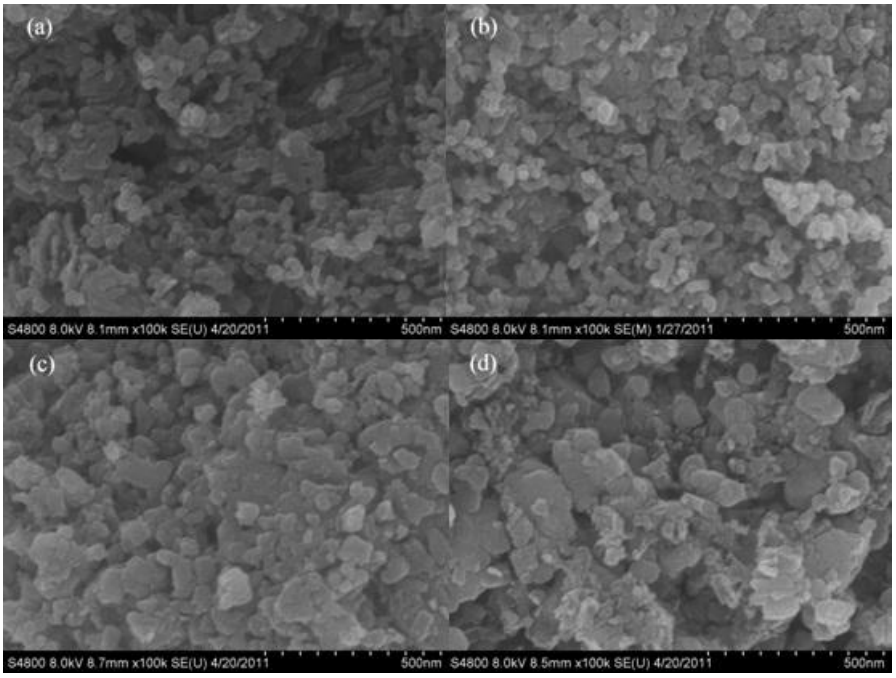

Figure 4. Scanning electron microscopy images of Li_2MnSiO_4 prepared at (a) 550ºC, (b) 600ºC, (c) 650ºC, (d) 700ºC

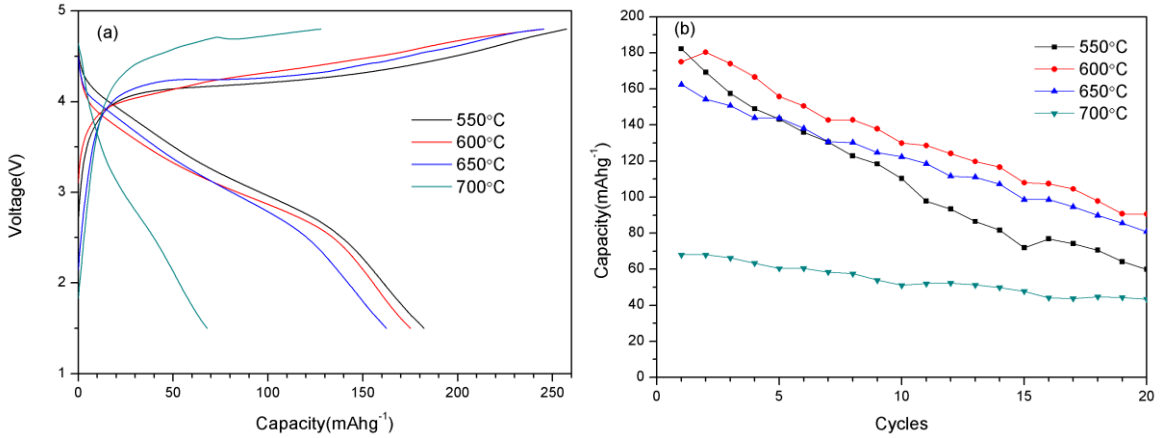

Figure 5. The cell performance of Li_2MnSiO_4 cathode materials prepared under various temperatures (a) initial charge-discharge curves and (b)cycling profiles

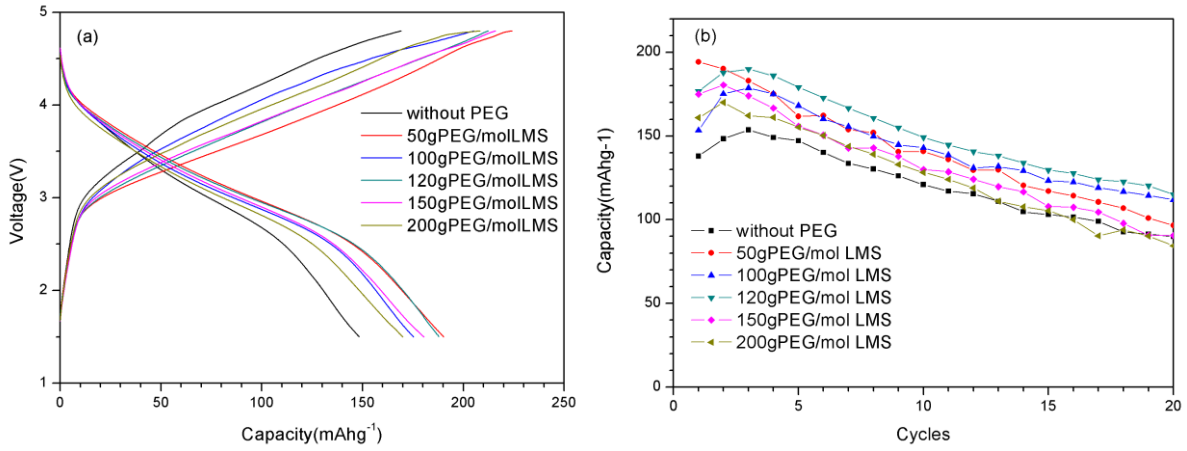

Figure 6. The cell performance of Li_2MnSiO_4 cathode materials prepared under various PEG addition amounts (a) second charge-discharge curves and (b) cycling profiles

At the optimum calcination temperature, effect of PEG addition amount during the preparation of Li_2MnSiO_4 precursor was investigated. Fig.6 shows the influence of PEG amount on the discharge performance at the 30mA g^{-1} discharge current of samples synthesized at 600ºC. As shown in Fig. 6(b), the cells presented the highest discharge capacity of 154, 194, 179, 190, 180and 170mAh g^{-1} for 0, 50, 100,120, 150, and 200g PEG 10000 in preparation of 1mol LMS(abbr. of Li_2MnSiO_4) respectively. Most of the cells exhibited the highest discharge capacity at the second cycle, so the second charge-discharge curves were given in Fig. 6 (a). The addition of PEG can improve discharge capacity of Li_2MnSiO_4 significantly. The sample synthesized with 120g PEG exhibited the best discharge performance while PEG free Li_2MnSiO_4 materials exhibited the lowest discharge capacity.

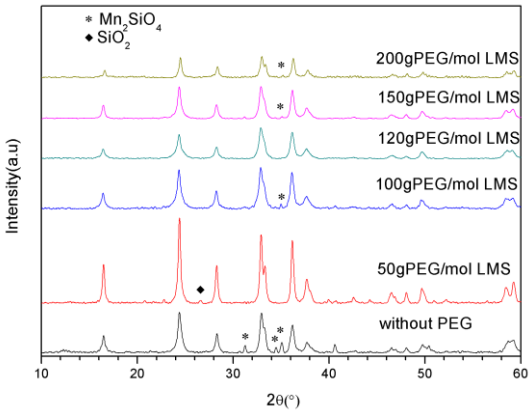

Figure 7. X-ray diffraction patterns of synthesized Li_2MnSiO_4 particles at different PEG addition amounts.

PEG was regarded as carbon source in synthesis of $LiFePO_4$ [25-27], so the influence of PEG amount on carbon concentration was determined in our research. As shown in Table 1, Elemental analysis indicated that carbon concentrations of all the samples were about 10%. PEG amount had little influence to carbon concentration. TG-curves shown in Fig.1 also showed that PEG lost 100% weight before 410 ºC. The carbon source was considered to be organic starting materials such as $Mn(CH_3COO)_2$ and $Si(OC_2H_5)_4$ instead of PEG. XRD was employed to study effect of PEG on phase structure. Fig.7 represents the series of powder X-ray diffraction patterns of synthesized Li_2MnSiO_4 at different PEG addition amounts. The Li_2MnSiO_4 sample prepared without PEG had the impurity phase Mn_2SiO_4. Addition of PEG can decrease the content of impurity phase apparently. In the Li_2MnSiO_4 sample prepared with 120g PEG/mol, Mn_2SiO_4 was avoided. During ball milling, PEG acted as a dispersant to make the slurry more uniform and stable. When the PEG addition amount increased to 150g/mol LMS or more, the slurry was difficult to dry and grind, which influenced the uniform of precursor powder.

Table 1. Properties of Li_2MnSiO_4 particles prepared at different PEG addition amounts

PEG amount (g/mol LMS)	BET Surface Area (m^2 g^{-1})	Carbon content (wt %)
0	43.49	10.78
50	61.48	9.01
100	61.07	11.05
120	69.29	10.55
150	74.31	11.13
200	77.99	8.97

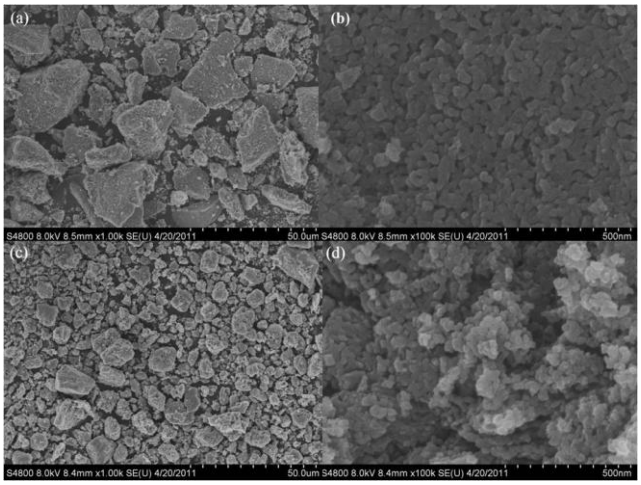

Figure 8. Scanning electron microscopy images of Li_2MnSiO_4 particles prepared at 600 ºC with different PEG amount. (a)(b) without PEG, (c)(d)PEG=120g/mol LMS.

As shown in table 1, BET surface area increased with the addition of PEG. Effect of PEG on morphology and particle size of Li_2MnSiO_4 powder was investigated by FE-SEM. As shown in Fig.8，the PEG free Li_2MnSiO_4 exhibited partially sintered primary particles which formed secondary particles with a large size range. The sample prepared with PEG showed partially agglomerated nonoparticles with an average particle size of 30-50nm. The primary particles aggregated to secondary particles with a size up to several μm. The smaller size of the primary particles with larger surface area improves the lithium ion and electronic conduction, which can improve the rate capability and cycling stability of materials[4,22]. It is obvious that PEG can prevent aggregation of Li_2MnSiO_4 and reduce the particle size of secondary particles and primary particles, which lead to improved electrochemical performance.

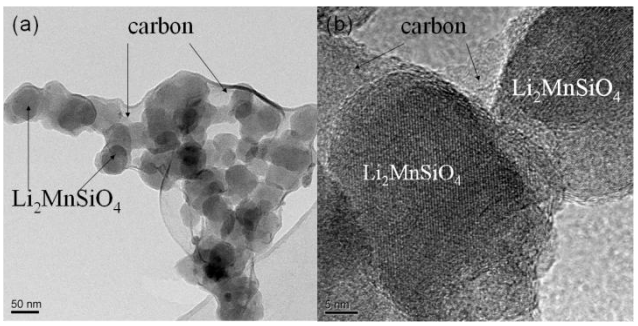

Figure 9. (a) Transmission electron microscopic and (b) high resolution-transmission electron microscopic image of Li_2MnSiO_4 /C nanoparticles prepared under optimized condition.

According to the above research, prepare condition was optimized as follows: the PEG amount was 120g/mol LMS, the calcination temperature was 600ºC. Fig.9 shows the TEM and HR-TEM images of Li_2MnSiO_4/C nanoparticles prepared under optimized condition,. TEM images showed that nanoparticles with an average particle size of ~50nm were coated with thin carbon layer on the surface.

HR-TEM showed that Li_2MnSiO_4 nanocrystals were coated by amorphous carbon. The small particle size of Li_2MnSiO_4 provides short pathways for rapid lithium-ion and electron conduction within the nanoparticles, while the carbon coating connects the nanoparticles in close proximity, providing a highly conductive channel for the electron mobility between adjacent Li_2MnSiO_4 nanoparticles[4].

To validate the effect of PEG on the electrical conductivity of Li_2MnSiO_4, electrochemical impedance spectroscopy (EIS) was utilized, which is a versatile electrochemical technique to characterize electrical properties of any material and its interface[21]. Fig. 10 illustrates EIS of Li_2MnSiO_4 cathode materials prepared with and without PEG. The measured EIS show single semicircles over the high frequency range, followed by short straight lines in the low frequency region for both samples. The diameter of the semicircle corresponds to the interfacial charge-transfer (CT) impedance. It is obvious that the diameter of semicircle for Li_2MnSiO_4 electrodes decreased with addition of PEG, which suggested lower CT impedance of electrodes. The electronic conductivity of Li_2MnSiO_4 materials has improved which attribute to smaller size of primary and secondary particles, as well as larger surface area coated by carbon.

Rate capability studies were also conducted to ensure the electrochemical activity at different current densities. Fig.11 represents the cycling profiles of Li_2MnSiO_4 prepared under the optimum condition at various current density from 10mA g^{-1} to 200mA g^{-1}. The Li/ Li_2MnSiO_4 cell delivered the highest discharge capacity of 204, 167 and 128 mAh g^{-1} at the current density 10 mA g^{-1}（1^{st} cycle）, 100 mA g^{-1} (3^{rd} cycle)and 200 mA g^{-1} (5^{th} cycle)in room temperature. At the 20^{th} cycle, the discharge capacity retained 105, 114 and 94mAh g^{-1} respectively. The discharge capacity at the current density 200 mA g^{-1} retained 84 % of the initial capacity at the 20^{th} cycle. Thus an increase in the charge/discharge current density did not lead to large decrease in capacity, even improved the cycle performance, which suggested that Li_2MnSiO_4 is a promising cathode materials with high capacity.

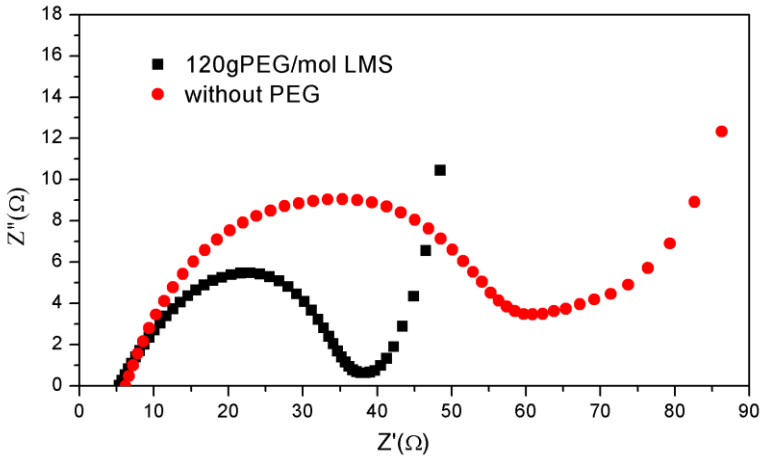

Figure 10. Electrochemical impedance spectroscopy of Li_2MnSiO_4 cathode prepared with or without PEG.

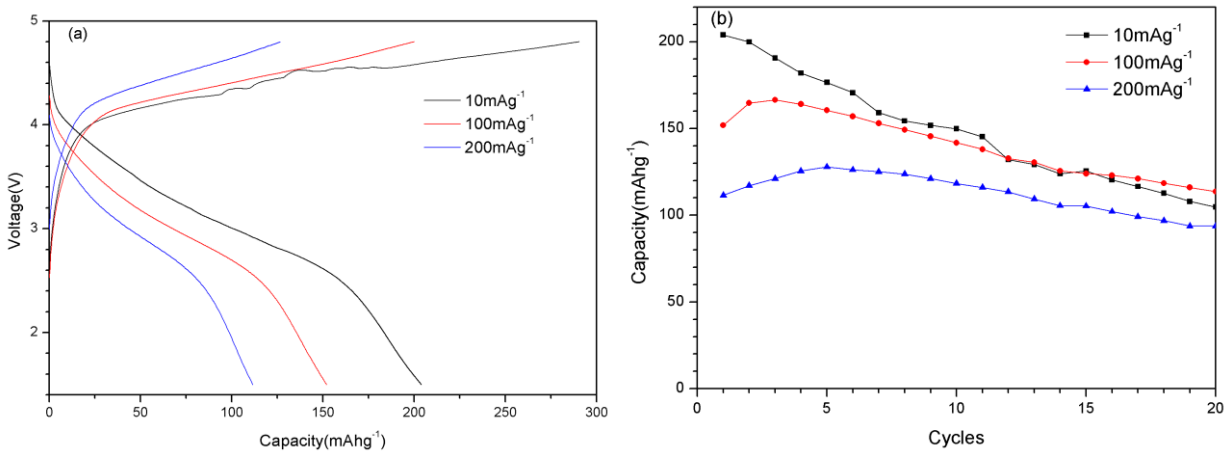

Figure 11. The cell performance of Li_2MnSiO_4 cathode materials under various current densities. (a) Initial charge-discharge curves and (b) cycling profiles

4. CONCLUSIONS

In summary, we have demonstrated the synthesis of carbon- coated Li_2MnSiO_4 by a PEG assisted solid-state reaction method. The calcination temperature and PEG addition amount were optimized, and their effects on phase purity, surface morphology as well as electrochemical performance were studied. Phase pure Li_2MnSiO_4 with orthorhombic structure was prepared at 700ºC. The Li_2MnSiO_4 prepared with 120g PEG/mol LMS and calcined at 600ºC exhibited initial discharge capacity 204mAhg^{-1} at the current density 10 mA g^{-1} at room temperature. HR-TEM confirmed that Li_2MnSiO_4 nanocrystals were coated by amorphous carbon. PEG played an important role, not as carbon source but as dispersant and to make the slurry more homogeneous and stable during ball milling so as to achieve phase pure material. PEG also had positive effect on morphology and particle size distribution. The carbon source was organic materials themselves. Reduction in particle size and coating with carbon improved electronic conductivity of Li_2MnSiO_4, therefore the cell electrochemical performance was improved significantly.

ACKNOWLEDGEMENTS
This work was financially supported by Scientific Research Fund of Zhejiang Provincial Education Department (Y201119941) and National Natural Science Foundation of China (21103212) .

References

1. M. E. A. de Dompablo, M. Armand, J .M. Tarascon, U. Amador, *Electrochem. Commun.*, 8(2006) 1292.
2. V. Aravindan, K. Karthikeyan, S. Ravi, S. Amaresh, W. S. Kim, Y. S. Lee, *J. Mater. Chem.*, 20(2010) 7340.
3. C. Lyness, B. Delobel, A. R Armstrong, P. G. Bruce, *Chem. Commun.*, 46(2007) 4890.
4. T. Muraliganth, K. R. Stroukoff, A. Manthiram, *Chem. Mater.*, 22(2010) 5754.

5. C. Deng, S. Zhang, B. L. Fu, S. Y. Yang, L. Ma, *Mater. Chem. Phys.*, 120(2010) 14.
6. A. Nytén, A. Abouimrane, M. Armand, T. Gustafsson, J.O.Thomas, *Electrochem. Commun.*,7(2005) 156.
7. S. I. Nishimura, S. Hayese, R. Kanno, M. Yashima, N. Nakayama, A. Yamada, *J. Am. Chem. Soc.*, 130(2008) 13212.
8. R. Dominko, M. Bele, M. Gaberšček, A. Meden, M. Remškar, J. Jamnik, *Electrochem. Commun.*, 8(2006)217.
9. R. Dominko, *J. Power Sources*, 184(2008) , 462.
10. X.Y. Fan, Y. Li, J.J. Wang, L. Gou, P. Zhao, D. L. Li, L. Huang, S.G. Sun, *J. Alloys. Compd.*, 493(2010) 77.
11. K. Karthikeyan, V. Aravindan, S.B. Lee, I.C. Jang, H.H. Lim, G.J. Park, M. Yoshioc,Y.S. Lee, *J. Alloys. Compd.*,504(2010)224.
12. B. Huang, X. Zheng, M. Lu,*J. Alloys. Compd.*,525 (2012) 110.
13. Z. Yan, S. Cai, L. Miao, X. Zhou, Y. Zhao, *J. Alloys. Compd.*,511 (2012) 101.
14. V. Aravindan, S. Ravi, W.S. Kim, S.Y. Lee, Y.S. Lee, *J. Colloid Interf. Sci.*, 355(2011)472.
15. P.Ghosh, S. Mahanty, R. N. Basu,*J. Electrochem. Soc.*, 156(2009) A677.
16. K. Karthikeyan, V. Aravindan, S. B. Lee, I. C. Jang, H. H. Lim, G. J. Park, M. Yoshio, Y. S. Lee, *J. Power Sources*, 195(2010) 3761.
17. W. Liu, Y. Xu, R. Yang, *J. Alloys. Compd.*, 480(2009) L1.
18. I. Belharouak, A. Abouimrane, K. Amine, *J. Phys. Chem. C.*, 113(2009) 20733.
19. Y. X. Li, Z. L. Gong,d Y. Yang, *J. Power Sources.*, 174(2007) 528.
20. M. E. A. de Dompablo, R. Dominko, J. M. G. Amores, L. Dupont, G. Mali, H. Ehrenberg, J. Jamnik, E. Moran, *Chem. Mater.*, 20(2008) 5574.
21. V. Aravindan, K. Karthikeyan, K. S. Kang, W. S. Yoon, W. S. Kim, Y. S. Lee, *J. Mater. Chem.*, 21(2011) 2470.
22. X.Kong, T.Mei, Z. Xing, N. Li, Z. Yuan, Y. Zhu, Y. Qian,*Int. J. Electrochem. Sci.*, 7 **(2012)** 5565
23. C. Deng, Y. H. Sun, S. Zhang, H. M. Lin, Y. Gao, B. Wu, L. Ma, Y. Shang, G. Dong, *Int. J. Electrochem. Sci.*, 7 **(2012)** 4559
24. M. K. Devaraju, R. Dinesh, H. Itaru, *Chem. Commun.*, 48(2012) 2698.
25. Z. Xu, L. Xu, Q. Lai, X. Ji, *Mater. Res. Bull.*, 42(2007) 883.
26. G. T. K. Fey, K. P. Huang, H.M. Kao, W. H. Li, *J. Power Sources*, 196(2011)2810.
27. L. N. Wang, X. C. Zhan, Z. G. Zhang, K. L. Zhang, *J. Alloys and Compd.*, 456(2008) 461.
28. A. Boulineau, C. Sirisopanaporn, R. Dominko, A. R. Armstrong,P. G. Bruce and C. Masquelier, *Dalton Trans.*, 39(2010) 6310.